Low-spin Fe in silicate perovskite and a possible layer at the base of the lower mantle

C. Mccammon, L. Dubrovinsky, O. Narygina, I. Kantor, X. Wu, K. Glazyrin, I. Sergueev, A.I. Chumakov

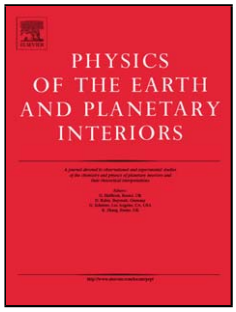

Title: Low-spin Fe^{2+} in silicate perovskite and a possible layer at the base of the lower mantle

Authors: C. McCammon, L. Dubrovinsky, O. Narygina, I. Kantor, X. Wu, K. Glazyrin, I. Sergueev, A.I. Chumakov

PII: S0031-9201(09)00222-2
DOI: doi:10.1016/j.pepi.2009.10.012
Reference: PEPI 5220

To appear in: *Physics of the Earth and Planetary Interiors*

Received date: 2-6-2009
Revised date: 6-10-2009
Accepted date: 29-10-2009

Please cite this article as: McCammon, C., Dubrovinsky, L., Narygina, O., Kantor, I., Wu, X., Glazyrin, K., Sergueev, I., Chumakov, A.I., Low-spin Fe^{2+} in silicate perovskite and a possible layer at the base of the lower mantle, *Physics of the Earth and Planetary Interiors* (2008), doi:10.1016/j.pepi.2009.10.012

Low-spin Fe^{2+} in silicate perovskite and a possible layer at the base of the lower mantle

C. McCammon[1*], L. Dubrovinsky[1], O. Narygina[1], I. Kantor[1,2], X. Wu[1], K. Glazyrin[1], I. Sergueev[3], A. I. Chumakov[3]

[1]Bayerisches Geoinstitut, Universität Bayreuth, D-95440 Bayreuth, Germany
[2]now at: University of Chicago, CARS, Building 434A, 9700 S. Cass Avenue, Argonne, IL, 60439, USA
[3]European Synchrotron Radiation Facility, BP 220, F-38043 Grenoble Cedex, France

*corresponding author
e-mail: catherine.mccammon@uni-bayreuth.de
fax: +49-(0)921-553769

Abstract

We investigated the spin state of iron in $Mg_{0.82}Fe_{0.18}SiO_3$ silicate perovskite using Mössbauer spectroscopy and nuclear forward scattering (NFS) at pressures up to 130 GPa and temperatures up to 1000 K. Majorite starting material was loaded into diamond anvil cells in three separate experiments, and transformed to silicate perovskite through laser heating. We found, in agreement with previous work, the predominance of a component with high isomer shift (~ 1 mm/s relative to α-Fe) and high quadrupole splitting (QS) (> 4 mm/s) in Mössbauer and NFS spectra up to 115 GPa at room temperature, and in accordance with previous work this component was assigned to intermediate-spin Fe^{2+}. At higher pressures, the intensity of the high QS component in the silicate perovskite spectrum decreased, while the intensity of a new component with low isomer shift (~ 0 mm/s relative to α-Fe) and low quadrupole splitting (< 0.5 mm/s) increased. This new component was assigned to low-spin Fe^{2+}, and its intensity increased with both increasing pressure and increasing temperature: at 120 GPa and 1000 K all Fe^{2+} was in the low-spin state. X-ray diffraction data showed well crystallised perovskite in all runs, and although the stable phase above ~ 110 GPa is expected to be post-perovskite, sluggish transition kinetics likely preserved the perovskite phase in a metastable state. Our results combined with data in the literature and thermodynamic and topological considerations suggest that there

may be a region where silicate perovskite containing low-spin Fe^{2+} is stable, which coincides with predicted pressure-temperature conditions near the D´´ layer.

Keywords: spin transition; D" layer; perovskite; post-perovskite; Mössbauer spectroscopy, nuclear forward scattering

1. Introduction

The base of the lower mantle shows many anomalous properties, a number of which have been explained by the transition of $(Mg,Fe)(Si,Al)O_3$ perovskite to a post-perovskite structure (e.g., Hirose, 2006). Other properties, however, remain unexplained (e.g., large P-wave velocity discontinuities, the sharpness of the D´´ discontinuity in some regions, high electrical conductivity and the nature of ultralow velocity layers). One possibility that has been considered to account for these observations is lateral variations in chemistry at the base of the lower mantle (Hirose et al., 2006). However there is another mechanism that can change physical and chemical properties of minerals, namely spin-pairing transitions of iron. Such transitions were predicted to occur within the Earth's interior nearly 50 years ago, but only in the past few years has direct experimental evidence for such transitions at lower mantle conditions been reported. For (Mg,Fe)O, both experimental and computational results confirm a high-spin to low-spin transition of Fe^{2+} that is expected to occur in the middle part of the lower mantle (e.g., Lin and Tsuchiya, 2008 and references therein). For $(Mg,Fe)(Si,Al)O_3$ perovskite, previous experimental results show a high-spin to intermediate-spin transition of Fe^{2+} that is expected to occur at the top of the lower mantle, with Fe^{2+} remaining in the intermediate-spin state throughout the bulk of the lower mantle (McCammon et al., 2008; Lin et al., 2008). Fe^{2+} in $(Mg,Fe)(Si,Al)O_3$ post-perovskite is also observed to be in the intermediate-spin state (Lin et al., 2008). However Badro et al. (2004) observed that iron in $(Mg,Fe)SiO_3$ perovskite was in the low-spin state above 120 GPa at room temperature, although since the post-perovskite phase had not been discovered when the experiments were performed, the structure of the sample was not investigated. To address the question of whether low-spin Fe^{2+} is stable in silicate perovskite, we conducted a combined nuclear forward scattering (NFS) and conventional Mössbauer experiment on $(Mg,Fe)SiO_3$ perovskite at high pressure and high temperature.

2. Experimental methods

The starting material for the present study was polycrystalline majorite with composition $Mg_{0.82}Fe_{0.18}SiO_3$ (~ 90% enriched in ^{57}Fe) (sample U1219; McCammon and Ross, 2003). The majorite sample was synthesised using a multianvil press; further details of synthesis conditions and sample characterisation can be found in McCammon and Ross (2003). We synthesised silicate perovskite from majorite using

a laser-heated diamond anvil cell (DAC) in three different experiments, and carried out Mössbauer spectroscopy and/or NFS measurements over a range of different pressures and temperatures. The run conditions are summarised in Table 1.

Run #1 was carried out at the European Synchrotron Radiation Facility (ESRF) during experiment HE-2750. The majorite sample was loaded together with a small ruby chip and a small (about 5 μm in diameter) piece of gold (used as a pressure marker) with thin layers of SiO_2 (which act as a thermal insulator during laser heating) into a Be gasket indented to ~ 20 μm thickness and drilled with a ~ 80 μm hole. The gasket was mounted within a panoramic-type DAC, designed and constructed at Bayerisches Geoinstitut for nuclear inelastic scattering (NIS) experiments, and equipped with bevelled 120 μm diameter culet gem-quality diamonds. The majorite sample was compressed to 33 GPa, and then heated with a double-sided near infrared laser (λ = 1064 nm) at temperatures between 1800 and 2000 K to transform the sample to silicate perovskite. Pressure was increased incrementally, with annealing after each increase of pressure using an infrared laser at low power (temperature peak around 1500 K) to relieve stress. The pressure was measured after each NFS spectrum using an online MAR CCD detector and calculated based on the equation of state of gold (Fei et al., 2007). NIS data were also collected during this experiment, but the results will be reported elsewhere.

Run #2 was carried out mainly at Bayerisches Geoinstitut, but with laser heating at ESRF and X-ray diffraction collected at the Advanced Photon Source (APS), USA. The majorite sample with thin layers of SiO_2 was loaded with a small ruby chip into a Re gasket preindented to about 30 μm thickness and drilled with a ~ 60 μm diameter hole, and mounted in a four-pin modified Merrill-Bassett DAC with 120 μm diameter culet gem-quality bevelled diamonds. The majorite sample was compressed in several steps to a pressure within the post-perovskite stability field, with annealing after each increase of pressure using an infrared laser at low power to relieve stress. At the highest pressure (145 ± 10 GPa according to ruby fluorescence and the Raman shift of diamond) the sample was heated with a Nd:YLF laser (λ = 1064 nm) to transform the sample to silicate perovskite. X-ray diffraction data collected on beamline IDD-13D at APS showed the sample to consist entirely of silicate perovskite at a pressure of 125 ± 5 GPa (based on the equation of state of silicate perovskite determined using the same methods; McCammon et al., 2008), with no evidence for a post-perovskite phase.

Run #3 was carried out primarily at ESRF during experiment HE-2750. Majorite was loaded together with a small ruby chip, a small piece of gold and layers of SiO_2 into a Re gasket as for run #1, and mounted in a four-pin modified Merrill-Bassett DAC with 200 μm diameter culet gem-quality bevelled diamonds that was fitted with an external resistive heater (Dubrovinskaia and Dubrovinsky, 2003). The majorite sample was compressed directly to 120 ± 5 GPa, where it was then heated with a near infrared laser to transform the sample to silicate perovskite. Subsequently the temperature was increased using the resistive heater, and the tension screws of the DAC were tightened to maintain the pressure at ~ 120 GPa during heating. Temperature was measured continuously using a S-type thermocouple mounted next to the diamonds, while pressure was measured both before and after the NFS data collection using ruby fluorescence corrected for temperature (Rekhi et al., 1999). A final NFS spectrum was collected after cooling to room temperature, and a Mössbauer spectrum was collected after return to Bayerisches Geoinstitut. High-resolution X-ray diffraction data were recorded on beam line ID09 at ESRF, and showed the sample to consist only of silicate perovskite plus a small amount of gold and SiO_2 (Fig. 1). The pressure was calculated from the X-ray diffraction pattern to be 130 ± 5 GPa based on the gold equation of state (Fei et al., 2007). The higher pressure on cooling likely resulted from the tightening of the tension screws during heating to maintain the pressure.

^{57}Fe Mössbauer spectra were recorded at room temperature in transmission mode on a constant acceleration Mössbauer spectrometer with a nominal 370 MBq ^{57}Co high specific activity source in a 12 μm thick Rh matrix. The methodology of high-pressure Mössbauer measurements is further described in McCammon et al. (1992) and Kantor et al. (2004). The velocity scale was calibrated relative to 25 μm thick α-Fe foil using the positions certified for (former) National Bureau of Standards standard reference material no. 1541; line widths of 0.36 mm/s for the outer lines of α-Fe were obtained at room temperature. The dimensionless effective thickness for the majorite sample measured in air was 2 (~ 5 mg unenriched Fe/cm^2), while for the majorite/perovskite in the DAC it was 24 (~ 52 mg unenriched Fe/cm^2). Spectra took 4 to 10 days each to collect. Mössbauer spectra were fitted to Lorentzian lineshapes in the thin-absorber approximation using conventional constraints (equal quadrupole component widths and areas) using the commercially available fitting program NORMOS written by R.A. Brand (distributed by Wissenschaftliche Elektronik

GmbH, Germany). To explore the influence of thickness effects, we additionally used a full transmission integral to fit the Mössbauer data, but found that hyperfine parameters and relative areas were unchanged within experimental uncertainty.

NFS data were collected on beamline ID18 at the ESRF during operation in 4-bunch mode, with the beam focused to ca. 8 μm × 13 μm using a Kirkpatrick-Baez mirror. Further details of the beamline are given in Rüffer and Chumakov (1996). All of the NFS spectra in run #3 and several of the spectra in run #1 were taken with the DAC in "vertical" geometry, i.e., with the plane of the gasket perpendicular to the X-ray beam. For the NFS spectra in run #1 that were taken in "horizontal" geometry, the X-ray beam passed through the Be gasket before reaching the sample. Each NFS spectrum took 1-2 hours to collect, and data were fitted using the program MOTIF (Shvyd'ko, 2000).

High-resolution X-ray diffraction data were collected at beamline ID09 at ESRF and beamline 13-ID-D at APS using the methods described in McCammon et al. (2008). X-ray patterns were analysed by Rietveld refinement using the GSAS package (Larsen and von Dreele, 1985).

3. Results

The NFS and Mössbauer spectra are illustrated in Figs. 2-4. In fitting the NFS spectra, our goal was to extract only the parameters that could be robustly derived from the data. We therefore restricted the number of sites to two, and varied only the following parameters during the fit (number of parameters indicated in parentheses): vertical scaling factor (1), Lorentzian broadening of all transitions (1), relative site proportion (1), relative isomer shift between sites (1), and quadrupole splitting of each site (2). Despite the limited parameter set, we were able to obtain reasonable fits for all spectra. Our goal was the same in fitting the Mössbauer spectra, but the energy-domain experiment enabled a larger number of parameters to be robustly determined from the data (although energy resolution of NFS is formally ideal, in practice it is limited by the time window of the 4-bunch mode = 704 ns, providing $\Delta E = \sim 0.1\ \Gamma_0$). The parameters determined from the Mössbauer spectra were: baseline (2); linewidth, isomer shift, quadrupole splitting and relative area for each site (4 for each site).

The zero-pressure NFS spectrum of majorite (Fig. 2a) is dominated by quantum beats with high frequency that arise from high-spin Fe^{2+} on the dodecahedral site, which is seen in the zero-pressure Mössbauer spectrum as a quadrupole doublet with

large splitting (Fig. 3a). The minor quadrupole doublets in the Mössbauer spectrum corresponding to high-spin Fe^{2+} on the octahedral site (~ 10%) and to high-spin Fe^{3+} (15-20%) (Fig. 3a) cause small modulations of the dominant quantum beats in the NFS spectrum (Fig. 2a), but the overall structure of the spectrum remains the same. The transition from majorite to silicate perovskite causes a significant change in the NFS spectrum (Fig. 2c), which resembles those reported at similar conditions by McCammon et al. (2008). There are several contributions dominated by a mixture of high-spin Fe^{2+} and intermediate-spin Fe^{2+}, both occupying the A site (McCammon et al., 2008). Since the high-spin Fe^{2+} contribution consists of more than one component, the use of only two components (one high-spin Fe^{2+} and one intermediate-spin Fe^{2+}) to fit the spectrum produces only a moderately good fit to the data (Fig. 2c). However the fit improves as the relative proportion of the high-quadrupole splitting component assigned to intermediate-spin Fe^{2+} increases with pressure (Fig. 2d), and at 115 GPa intermediate-spin Fe^{2+} accounts for nearly all of the spectrum (Fig. 2e). There is likely still a minor contribution from Fe^{3+}, which for this composition is estimated to be 15-20% $Fe^{3+}/\Sigma Fe$ (McCammon et al., 2004). However previous work has shown that the proportion of Fe^{3+} does not change significantly with pressure (Jackson et al., 2005; McCammon et al., 2008), and the results of the current study are also consistent with this observation.

The Mössbauer spectrum for majorite in the DAC is significantly reduced in quality from the zero-pressure spectrum (Fig. 3a) due to solid angle reduction and absorption by the diamonds; however the dominant quadrupole doublet due to high-spin Fe^{2+} on the dodecahedral site can still be resolved (Fig. 3b). After laser heating at ~ 145 GPa to transform the sample to silicate perovskite (structure confirmed by X-ray diffraction), there is a clear change in the spectrum (Fig. 3c). The quadrupole splitting of the dominant doublet increases, consistent with the presence of intermediate-spin Fe^{2+}, and a second component appears with significantly lower quadrupole splitting and isomer shift.

The presence of the low quadrupole splitting component is also observed when majorite is transformed through laser heating to silicate perovskite at 120 GPa (Fig. 4). In the NFS spectra the presence of the high frequency quantum beats corresponding to intermediate-spin Fe^{2+} can still be observed (Fig. 4a), but they are superimposed on a relatively monotonous downward slope arising from a component with nearly zero quadrupole splitting. The proportion of the low quadrupole splitting

component grows with increasing temperature (as seen by the disappearance of the high frequency quantum beats), and at 1000 K the spectrum consists of only low quadrupole splitting components. With the disappearance of intermediate-spin Fe^{2+} in Figs. 4d and 4e, the presence of a minor amount of a second component with low quadrupole splitting can be resolved, which likely corresponds to Fe^{3+}. The Mössbauer spectrum taken of the same sample at the same conditions as Fig. 4e shows the low quadrupole splitting component as a singlet with extremely low isomer shift (Fig. 3d), where the data scatter is too high for a Fe^{3+} component with ~ 20% abundance to be resolved. The X-ray diffraction pattern taken of the same sample as Fig. 3d shows only the *Pbnm* perovskite structure, confirming that the new component arises only from an electronic transition (Fig. 1).

The variation of hyperfine parameters with pressure shows consistent trends for the different components in the Mössbauer and NFS spectra (Fig. 5). The most notable feature is the appearance above 120 GPa of the component with low isomer shift and quadrupole splitting. The proportion of this component increases correspondingly with the decrease of intermediate-spin Fe^{2+}, and there is a large difference in isomer shift between this component and intermediate-spin Fe^{2+} (Fig. 5). The most plausible assignment for this component is low-spin Fe^{2+} in the A site of silicate perovskite, which is predicted to have both low isomer shift and low quadrupole splitting (e.g., Li et al., 2006 and references therein). The proportion of low-spin Fe^{2+} in silicate perovskite increases with both increasing pressure and increasing temperature (Fig. 6).

The assignment of the low quadrupole splitting component to low-spin Fe^{2+} is also consistent with X-ray emission data which show a nearly complete disappearance of the Kβ' satellite peak above 120 GPa, indicating the complete spin pairing of 3*d* electrons (the residual intensity can be accounted for by a small amount of Fe^{3+}) (Badro et al., 2004). Electrical conductivity data of $Mg_{0.9}Fe_{0.1}SiO_3$ perovskite also support the interpretation of low-spin Fe^{2+}. The conductivity drop of more than two orders of magnitude between 58 and 104 GPa (Ohta et al., 2008) follows the expected behaviour of a transition from two unpaired electrons (intermediate-spin Fe^{2+}) to none (low-spin Fe^{2+}).

Low-spin Fe^{2+} has similar isomer shift and quadrupole splitting values to Fe^{3+} (Fig. 5), suggesting an alternative interpretation, namely that the low quadrupole splitting component in Fig. 4 could be due to Fe^{3+}. We consider such a possibility to be

unlikely, however. The growth in intensity of the low quadrupole splitting component is proportional to the decrease of the intermediate-spin Fe^{2+} component, indicating that both take part in the transition. We can rule out that oxidation of Fe^{2+} to Fe^{3+} takes place as part of a chemical reaction, because we found the transition to be fully reversible with both pressure and temperature. It is also unlikely that intervalence charge transfer takes place, such as in $FeTiO_3$ at high pressure ($Fe^{2+} + Ti^{4+} \leftrightarrow Fe^{3+} + Ti^{3+}$; Seda and Hearne, 2004) or (Mg,Fe,Cr)O at high temperature ($Fe^{2+} + Cr^{3+} \leftrightarrow Fe^{3+} + Cr^{2+}$; Eeckhout et al., 2007), since there are no other species in our experiments that could participate in coupled electron transfer. We can also rule out that the low quadrupole splitting component could arise through the reaction $Fe^{2+} \rightarrow Fe^{3+} + Fe^{0}$ as recently reported by Jackson et al. (2009) for laser-heated DAC experiments with $(Mg,Fe)SiO_3$ post-perovskite, because we found the transition to be fully reversible with both pressure and temperature.

Previous NFS studies of $(Mg,Fe)SiO_3$ and $(Mg,Fe)(Si,Al)O_3$ perovskite have suggested that Fe^{3+} may undergo a pressure-induced spin transition (Jackson et al., 2005; Li et al., 2006). However the samples used in these studies contained appreciable amounts of Fe^{3+} ($Fe^{3+}/\Sigma Fe \sim 0.4$ and 0.5 for the Jackson et al. and the Li et al. samples, respectively) compared to the present study ($Fe^{3+}/\Sigma Fe \sim 0.15$-0.2). Due to the low intensity of the Fe^{3+} component in our data, we cannot resolve the behaviour of Fe^{3+} unambiguously; hence the question of a spin transition in Fe^{3+} must remain open. We note, however, that our conclusions are independent of the behaviour of Fe^{3+}, and they would not change if there were a spin transition in that component.

Umemoto et al. (2008) suggested that sample annealing could enhance cation diffusion and clustering of irons at high pressure, which would promote the stability of low-spin Fe^{2+} in silicate perovskite. However since our experiment involving external heating (run #3) was conducted after the sample was laser heated *at the same pressure* to synthesise silicate perovskite, the degree of cation order would not have changed significantly during external heating. We therefore maintain that the spin state recorded by our measurements at 120 GPa and 1000 K represents close to equilibrium for those conditions.

Recent computational studies of iron in silicate perovskite have reported a pressure-induced high-spin to low-spin transition of Fe^{2+} in the A site (e.g., Stackhouse et al., 2007; Bengston et al., 2008; Umemoto et al., 2008). Pressure

determinations for the spin transition of silicate perovskite for the iron composition used in the present study range from ~ 60 GPa to ~ 200 GPa, depending on parameters such as the exchange correlation method used and the atomic configuration of iron atoms in the supercell.

4. Discussion

Our results show that an intermediate- to low-spin transition involving Fe^{2+} on the A site takes place in $Mg_{0.82}Fe_{0.18}SiO_3$ perovskite around 120 GPa. At this pressure the stable structure is expected to be post-perovskite (e.g., Hirose, 2006, and references therein); however the well known sluggish reaction kinetics of the perovskite to post-perovskite phase transition (e.g., Mao et al., 2004) likely preserved the perovskite structure in a metastable state in our experiments. The important question is, therefore, whether silicate perovskite with low-spin Fe^{2+} is thermodynamically stable in any region of the phase diagram.

Our experimental data demonstrate that increasing temperature increases the stability of low-spin Fe^{2+} in silicate perovskite, reaching 100% low-spin Fe^{2+} at 1000 K and 120 GPa (Fig. 6). It follows, therefore, that higher temperatures will preserve the low-spin state. If the phase boundary between perovskite and post-perovskite were shifted to higher pressures as a consequence of the intermediate- to low-spin transition of Fe^{2+} in silicate perovskite, there would be a region in which low-spin Fe^{2+} would be stable (Fig. 7). The slope of the phase boundary depends on the relative contribution of the entropy and volume terms to the free energy. Our observation that temperature stabilises the low-spin state relative to intermediate-spin Fe^{2+} implies that the P,T slope of the transition in the perovskite field is negative, which means that the low-spin Fe^{2+} perovskite to post-perovskite phase boundary must have a less steep slope than the intermediate-spin Fe^{2+} perovskite to post-perovskite phase boundary based on Schreinemakers' Rules (Schreinemakers, 1916).

Our proposed phase diagram is consistent with existing data on the spin state of Fe^{2+} in silicate perovskite (Fig. 7). Lin et al. (2008) collected X-ray emission spectra for $Mg_{0.6}Fe_{0.4}SiO_3$ perovskite at high pressure and temperature, and found a spin number (S) close to one up to 3200 K at 108 GPa, which is consistent with the nuclear forward scattering data of McCammon et al. (2008) for $Mg_{0.88}Fe_{0.12}SiO_3$ perovskite which showed intermediate-spin Fe^{2+} ($S = 1$) to be present at 110 GPa and 300 K. X-ray emission spectra of Badro et al. (2004) for $Mg_{0.9}Fe_{0.1}SiO_3$ perovskite showed a

spin number near one at 120 GPa, but near zero at 132 and 145 GPa. Lin et al. (2008) suggest that an iron content below $x_{Fe} = 0.4$ is likely below the percolation threshold where iron-iron interactions could significantly influence the spin transition pressure; hence no strong difference in spin behaviour would be predicted within the composition range of data shown in Fig. 7.

The pressure interval over which low-spin Fe^{2+} perovskite could occur coincides with predicted P,T conditions near D'', raising the possibility of a layer at the base of the lower mantle containing low-spin Fe^{2+}. Lateral temperature variations change the depth of the perovskite to post-perovskite transition, which would also affect the relative abundance of different spin-state populations. In hot regions the intermediate- to low-spin transition would occur well above the core-mantle boundary (CMB), while in cold regions silicate perovskite with intermediate-spin Fe^{2+} would transform directly to post-perovskite (Fig. 8). Hernlund et al. (2005) proposed that in cold regions above the core-mantle boundary a double crossing of the perovskite to post-perovskite transition could occur, accounting for double seismic discontinuities and allowing an estimate of heat flow out of the core. In our scenario a double crossing would still occur, but the layer of silicate perovskite adjoining the CMB would contain low-spin Fe^{2+}, not intermediate spin, which would influence physical and chemical properties in that region.

The double-crossing model has been used in conjunction with geophysically consistent estimates of deep mantle and inner core boundary temperatures to define plausible ranges for the Clapeyron slope of the perovskite to post-perovskite transition (Hernlund and Labrosse, 2007). In their analysis the higher estimates of the Clapeyron slope from experiment and theory gave the best agreement with estimates of core melting temperatures, while lower estimates such as those based on the gold pressure scale (e.g., Hirose, 2006) were judged to be inconsistent. According to our results, however, low-spin Fe^{2+} would increase the Clapeyron slope of the perovskite to post-perovskite transition significantly (Fig. 7), favouring lower inner core boundary temperatures and strengthening plausibility arguments for the double-crossing model (Hernlund and Labrosse, 2007).

5. Conclusions and outlook

Our work has shown that low-spin Fe^{2+} is stable in silicate perovskite above ~ 120 GPa, and that increasing temperature increases the stability of the low-spin state,

raising the possibility of a layer containing low-spin Fe^{2+} silicate perovskite in the lower mantle. The style of mantle convection is highly influenced by the chemical and physical properties of materials at the CMB; hence low-spin Fe^{2+} may play a role in mantle dynamics. Unfortunately little is known about the properties of silicate perovskite with low-spin Fe^{2+}, which means that assessment of geophysical implications must wait for the results of *in situ* studies, since spin transitions are reversible with respect to both pressure and temperature. An initial wish list includes measurements at conditions of D´´ of the spin state of iron in silicate perovskite as well as the Clapeyron slope of the perovskite to post-perovskite transition (Fig. 7), and the density change and sharpness of the intermediate- to low-spin transition in silicate perovskite.

Acknowledgements

We acknowledge the European Synchrotron Radiation Facility for provision of synchrotron radiation facilities (ID18 and ID09) and we would like to thank R. Rüffer and M. Hanfland for additional assistance. Use of the Advanced Photon Source (beamline 13-ID-D) was supported by the U.S. Department of Energy, Office of Science, Office of Basic Energy Sciences, under Contract No. DE-AC02-06CH11357, and we would like to thank Vitali Prakapenka for additional assistance. The project was partly supported by funds from the German Science Foundation (DFG) Priority Programme SPP1236 under project Mc 3/16-1.

References

Badro, J., Rueff, J.P., Vanko, G., Monaco, G., Fiquet, G. and Guyot, F., 2004. Electronic transitions in perovskite: Possible non-convecting layers in the lower mantle. Science, 305: 383-386.

Bengtson, A., Persson, K. and Morgan, D., 2008. *Ab initio* study of the composition dependence of the pressure induced spin crossover in perovskite $(Mg_{1-x},Fe_x)SiO_3$. Earth and Planetary Science Letters, 265: 535-545.

Dubrovinskaia, N. and Dubrovinsky, L., 2003. Whole-cell heater for the diamond anvil cell. Reviews of Scientific Instruments, 74: 3433-3437.

Eeckhout, S.G., Bolfan-Casanova, N., McCammon, C.A., Klemme, S. and Amiguet, E., 2007. XANES study of the oxidation state of Cr in lower mantle phases: periclase and magnesium silicate perovskite. American Mineralogist, 92: 966-972.

Fei, Y. et al., 2007. Toward an internally consistent pressure scale. Proceedings of the National Academy of Sciences of the United States of America, 104: 9182-9186.

Hernlund, J.W. and Labrosse, S., 2007. Geophysically consistent values of the perovskite to post-perovskite transition Clapeyron slope. Geophysical Research Letters, 34: doi:10.1029/2006GL028961, 2007.

Hernlund, J.W., Thomas, C. and Tackley, P.J., 2005. A doubling of the post-perovskite phase boundary and structure of the Earth's lowermost mantle. Nature, 434: 882-886.

Hirose, K., 2006. Postperovskite phase transition and its geophysical implications. Reviews of Geophysics, 44: RG3001.

Hirose, K., Karato, S, Cormier, V.F., Brodholt, J.P. and Yuen, D.A., 2006. Unsolved problems in the lowermost mantle. Geophysical Research Letters, 33: doi:10.1029/2006GL025691.

Jackson, J.M., Sturhahn, W., Shen, G., Zhao, J., Hu, M., Errandonea, D., Bass, J.D. and Fei, Y., 2005. A synchrotron Mössbauer spectroscopy study of (Mg,Fe)SiO_3 perovskite up to 120 GPa. American Mineralogist, 90: 199-205.

Jackson, J.M., Sturhahn, W., Tschauner, O., Lerche, M. and Fei, Y., 2009. Behavior of iron in (Mg,Fe)SiO_3 post-perovskite assemblages at Mbar pressures. Geophysical Research Letters, 36: doi:10.1029/2009GL037815.

Kantor, A.P., Jacobsen, S.D., Kantor, I.Y., Dubrovinsky, L.S., McCammon, C.A. and Reichmann, H.J., 2004. Pressure-induced magnetization in FeO: evidence from elasticity and Mössbauer spectroscopy. Physical Review Letters, 93: DOI: 10.1103/PhysRevLett.93.215502.

Larsen, A.C. and von Dreele, R.B., 1985. General Structure Analysis System (GSAS). Los Alamos National Laboratory Report LAUR B6-748, Los Alamos, USA.

Li, J., Sturhahn, W., Jackson, J.M., Struzhkin, V.V., Lin, J.F., Zhao, J., Mao, H.K. and Shen, G., 2006. Pressure effect on the electronic structure of iron in $(Mg,Fe)(Si,Al)O_3$ perovskite: a combined synchrotron Mössbauer and X-ray emission spectroscopy study up to 100 GPa. Physics and Chemistry of Minerals, 33: 575-585.

Lin, J.-F. and Tsuchiya, T., 2008. Spin transition of iron in the Earth's lower mantle. Physics of the Earth and Planetary Interiors, 170: 248-259.

Lin, J.-F., Watson, H., Vankó, G., Alp, E.E., Prakapenka, V.B., Dera, P., Struzhkin, V.V., Kubo, A., Zhao, J., McCammon, C. and Evans, W.J., 2008. Predominant intermediate-spin ferrous iron in lowermost mantle post-perovskite and perovskite. Nature Geoscience: 688-691.

Mao, W.L., Meng, Y., Shen, G., Prakapenka, V.B., Campbell, A.J., Heinz, D.L., Shu, J., Caracas, R., Cohen, R.E., Fei, Y., Hemley, R.J. and Mao, H.-k., 2005. Iron-rich silicates in the Earth's D" layer. Proceedings of the National Academy of Sciences, 102: 9751-9753.

McCammon, C.A., 1992. A new apparatus to conduct variable temperature high pressure Mössbauer spectroscopy. In: A.K. Singh (Editor), Recent Trends in High Pressure Research (Proceedings of the XIII AIRAPT International Conference on High Pressure Science and Technology). Oxford and IBL Publ. Co., New Dehli, India, pp. 824-826.

McCammon, C.A. and Ross, N.L., 2003. Crystal chemistry of ferric iron in $(Mg,Fe)(Si,Al)O_3$ majorite with implications for the transition zone. Physics and Chemistry of Minerals, 30: 206-216.

McCammon, C.A., Lauterbach, S., Seifert, F., Langenhorst, F. and van Aken, P.A., 2004. Iron oxidation state in lower mantle mineral assemblages I. Empirical relations

449 derived from high-pressure experiments. Earth and Planetary Science Letters, 222:
450 435-449.
451
452 McCammon, C., Kantor, I., Narygina, O., Rouquette, J., Ponkratz, U., Sergueev, I.,
453 Mezouar, M., Prakapenka, V. and Dubrovinsky, L., 2008. Stable intermediate-spin
454 ferrous iron in lower mantle perovskite. Nature Geoscience, 1: 684-687.
455
456 Ohta, K., Onoda, S., Hirose, K., Sinmyo, R., Shimizu, K., Sata, N., Ohishi, Y. and
457 Yasuhara, A., 2008. The electrical conductivity of post-perovskite in Earth's D" layer.
458 Science, 320: 89-91.
459
460 Rekhi, S., Dubrovinsky, L.S. and Saxena, S.K., 1999. Temperature-induced ruby
461 fluorescence shifts up to a pressure of 15 GPa in an externally heated diamond anvil
462 cell. High Temperatures - High Pressures, 31: 299-305.
463
464 Rüffer, R. and Chumakov, A.I., 1996. Nuclear resonance beamline at ESRF.
465 Hyperfine Interactions, 97/98: 589-604.
466
467 Schreinemakers, F.A.H., 1916. Invariant, monovariant and divariant equilibria.
468 Proceedings of the Academy of Science of Amsterdam, 19: 514-527.
469
470 Seda, T. and Hearne, G.R., 2004. Pressure induced Fe^{2+} + Ti^{4+} -> Fe^{3+} + Ti^{3+}
471 intervalence charge transfer and the Fe^{3+}/Fe^{2+} ratio in natural ilmenite ($FeTiO_3$)
472 minerals. Journal of Physics-Condensed Matter, 16: 2707-2718.
473
474 Shvyd'ko, Y.V., 2000. MOTIF: Evaluation of time spectra for nuclear forward
475 scattering. Hyperfine Interactions, 125: 173-188.
476
477 Stackhouse, S., Brodholt, J.P. and Price, G.D., 2007. Electronic spin transitions in
478 iron-bearing $MgSiO_3$ perovskite. Earth and Planetary Science Letters, 253: 282-290.
479
480 Umemoto, K., Wentzcovitch, R.M., Yu, Y.G. and Requist, R., 2008. Spin transition in
481 $(Mg,Fe)SiO_3$ perovskite under pressure. Earth and Planetary Science Letters, 276:
482 198-206.

Wysession, M.E., Lay, T., Revenaugh, J., Williams, Q., Garnero, E., Jeanloz, R. and Kellog, L., 1998. The D´´ discontinuity and its implications. In: M. Gurnis, M.E. Wysession, E. Knittle and B.A. Buffet (Editors), The Core-Mantle Boundary Region, Geodynamics Series 28. American Geophysical Union, Washington, DC, USA, pp. 231-253.

Figure Captions

Figure 1. X-ray diffraction pattern of silicate perovskite at room temperature and 130 (5) GPa collected at the end of run #3. The solid line through the data points indicates the fit derived from Rietveld refinement, and the line positions of Au (pressure marker), $CaCl_2$-structured SiO_2 (thermal insulator) and silicate perovskite with *Pbnm* space group are indicated by blue, red and black ticks, respectively.

Figure 2. Room temperature NFS spectra collected during run #1: (a) majorite in air at 0 GPa; (b) majorite in DAC at 33 GPa; (c-e) sample transformed to silicate perovskite by laser heating. The pressures for the spectra are as follows: (c) 40 GPa; (d) 62 GPa; (e) 115 GPa. The red lines indicate the theoretical fit obtained using MOTIF.

Figure 3. Room temperature Mössbauer spectra collected for (a) majorite in air (run #1); (b) majorite in the DAC (run #2); (c) (d) silicate perovskite in the DAC (runs #2 and #3). The pressures for the spectra are as follows: (a) 0 GPa; (b) 61 GPa; (c) 125 GPa; and (d) 130 GPa. The solid lines indicate the theoretical fit obtained using NORMOS, and the residual is indicated above each spectrum. The doublets are shaded as follows: high-spin Fe^{2+} (yellow); intermediate-spin Fe^{2+} (green); low-spin Fe^{2+} (blue); Fe^{3+} (red).

Figure 4. NFS spectra of silicate perovskite during run #3 (at P = 120 GPa unless otherwise noted): (a) T = 300 K; (b) T = 380 K; (c) T = 830 K; (d) T = 1000 K; (e) P = 130 GPa, T = 300 K. The NFS spectrum in Fig. 4e was collected for the same sample at the same conditions as the Mössbauer spectrum in Fig. 3d. The red lines indicate the theoretical fit obtained using MOTIF.

Figure 5. Hyperfine parameter variation with pressure for majorite and silicate perovskite derived from room temperature NFS (squares) and Mössbauer (circles) spectra. The trends for individual species are linked by solid and dashed lines in their regions of stability and metastability, respectively, for high-spin Fe^{2+} in majorite (yellow); intermediate-spin Fe^{2+} in perovskite (green); low-spin Fe^{2+} in perovskite (blue) and Fe^{3+} (red).

Figure 6. Proportion of low-spin Fe^{2+} relative to total Fe^{2+} in silicate perovskite as a function of temperature at high pressure based on NFS (squares) and Mössbauer (circles) spectra. The line joins the data for 120 GPa, while the pressures for the other data points are indicated.

Figure 7. Proposed phase boundary for $(Mg,Fe)(Si,Al)O_3$ between perovskite (pv) and post-perovskite (ppv). The thick solid line indicates the phase boundary summarised from data in the literature (Hirose, 2006), which may be shifted to higher pressures due to an intermediate-spin (IS) to low-spin (LS) transition in the perovskite phase, creating a region where silicate perovskite containing low-spin Fe^{2+} is stable (blue). The region where IS Fe^{2+} is stable in the perovskite structure is shaded yellow, while the region where IS Fe^{2+} is stable in the post-perovskite structure is shaded purple. Symbols indicate the spin state determined for Fe^{2+} in silicate perovskite, where green indicates intermediate spin and blue indicates low spin: large circles (this work); small circle (McCammon et al., 2008); diamonds (Lin et al., 2008); squares (Badro et al., 2004). The estimated depth range of the D´´ discontinuity is indicated by the black bar (e.g., Wysession et al., 1998), and the green and blue dashed lines are a guide for the eye.

Figure 8. The estimated thermal structure of D´´ adapted from Hernlund et al. (2005). The perovksite to post-perovksite transition is shown by the thick solid (existing data) and dashed (our proposed boundary) lines, and various geotherms are shown in red. The region where IS Fe^{2+} is stable in the perovskite structure is shaded yellow, while the region where IS Fe^{2+} is stable in the post-perovskite structure is shaded purple. The blue region is where silicate perovskite containing low-spin Fe^{2+} would be stable, which leads to the presence of post-perovskite lenses in cold regions (as already proposed by Hernlund et al., 2005), but with intermediate-spin Fe^{2+} silicate perovskite above and low-spin Fe^{2+} silicate perovskite below.

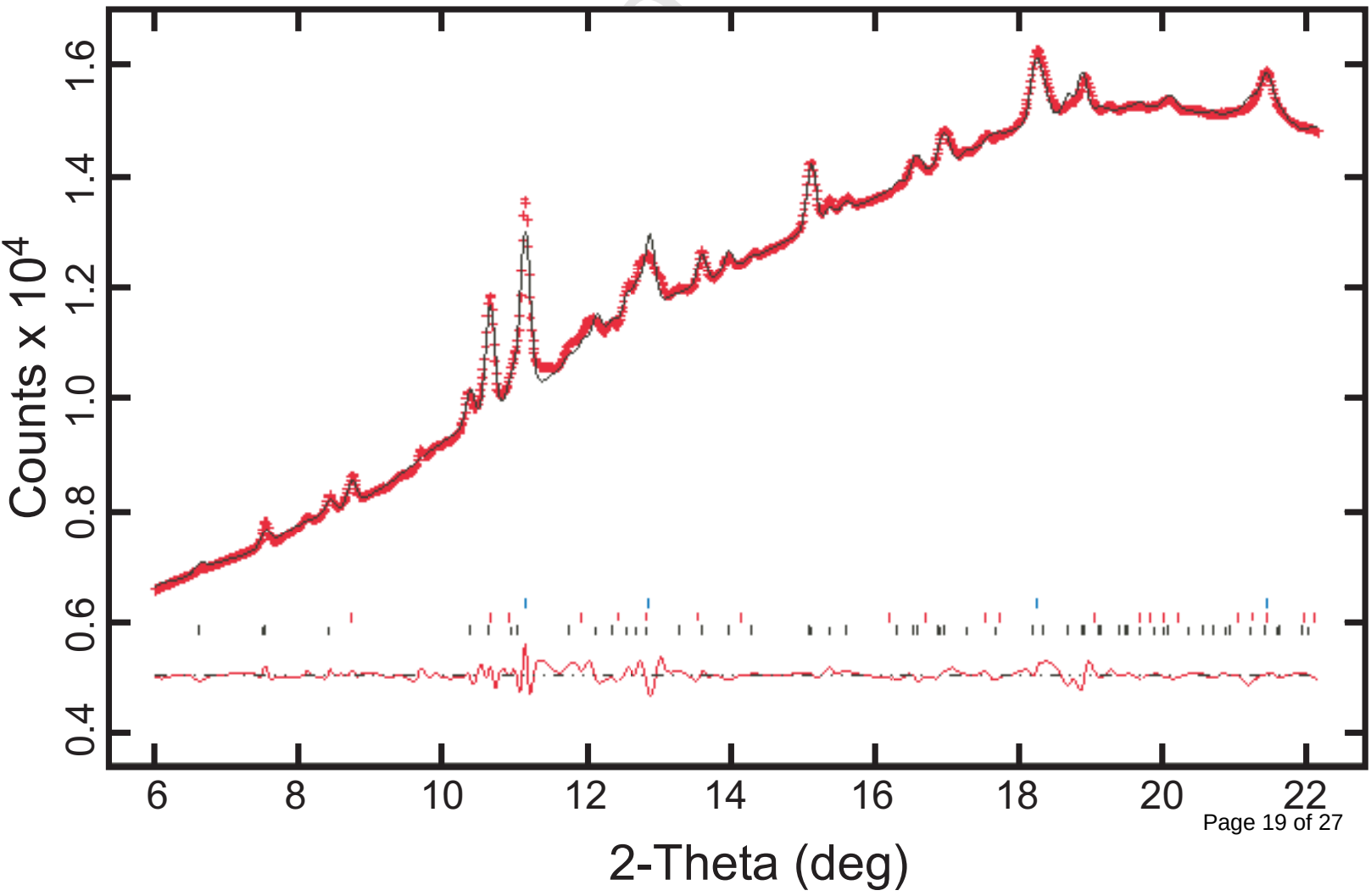

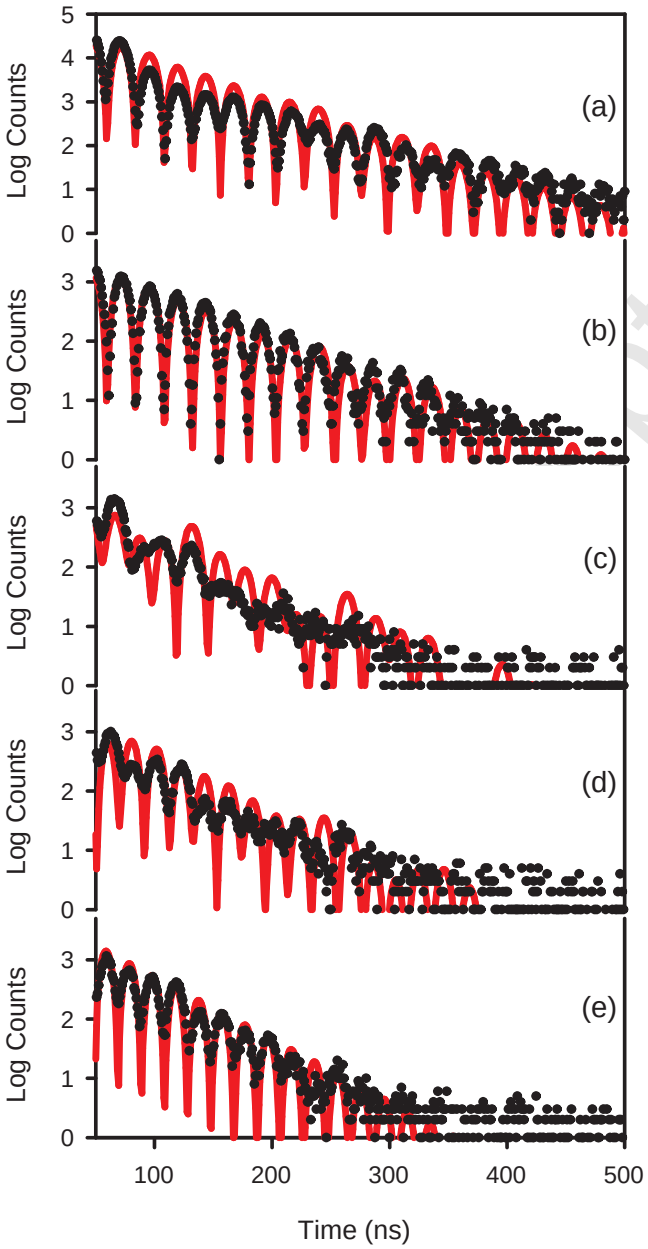

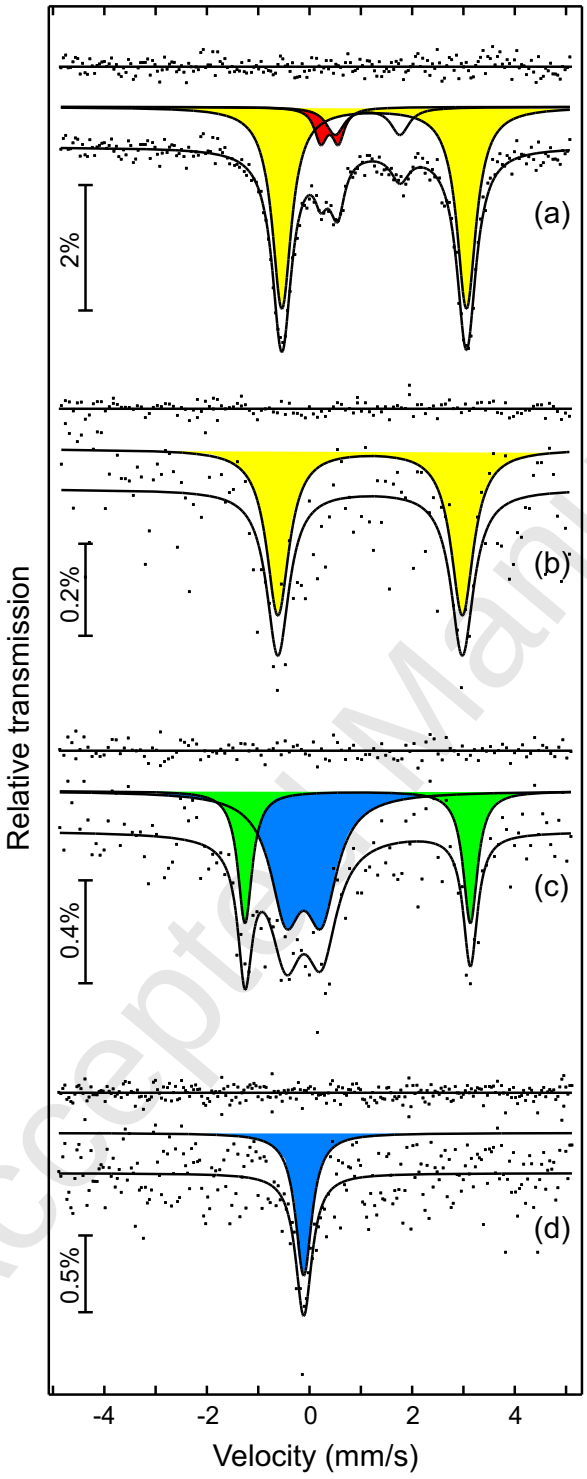

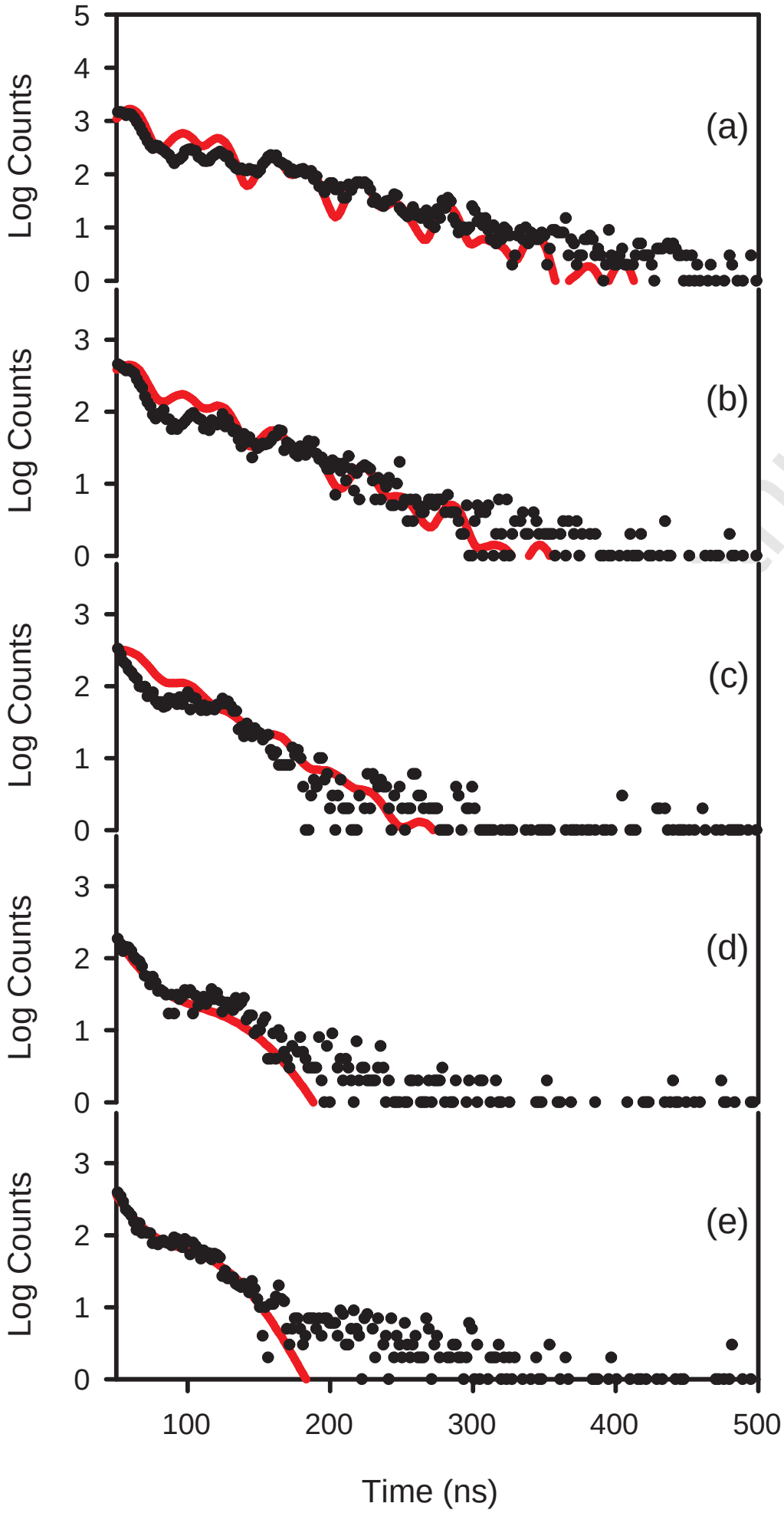

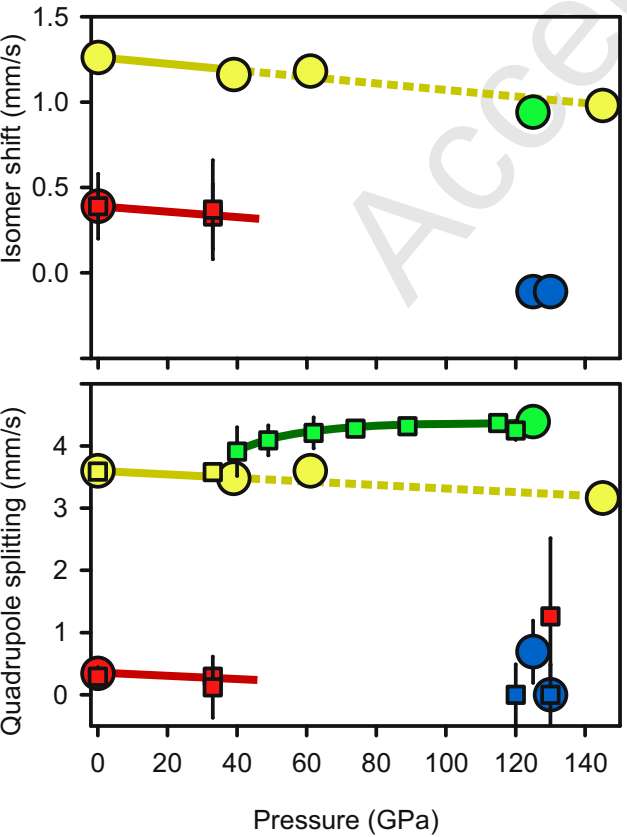

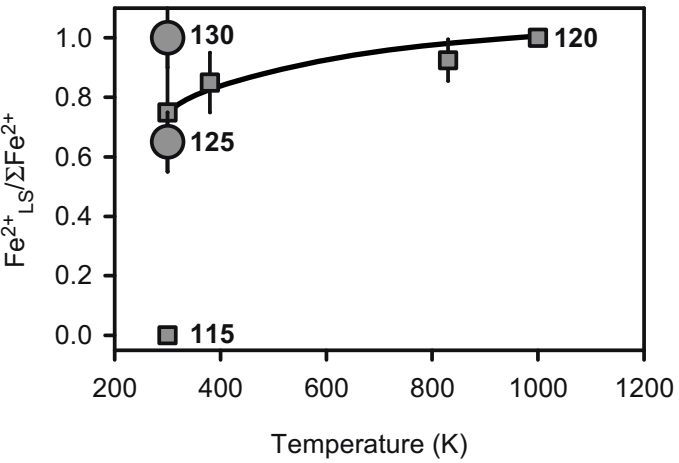

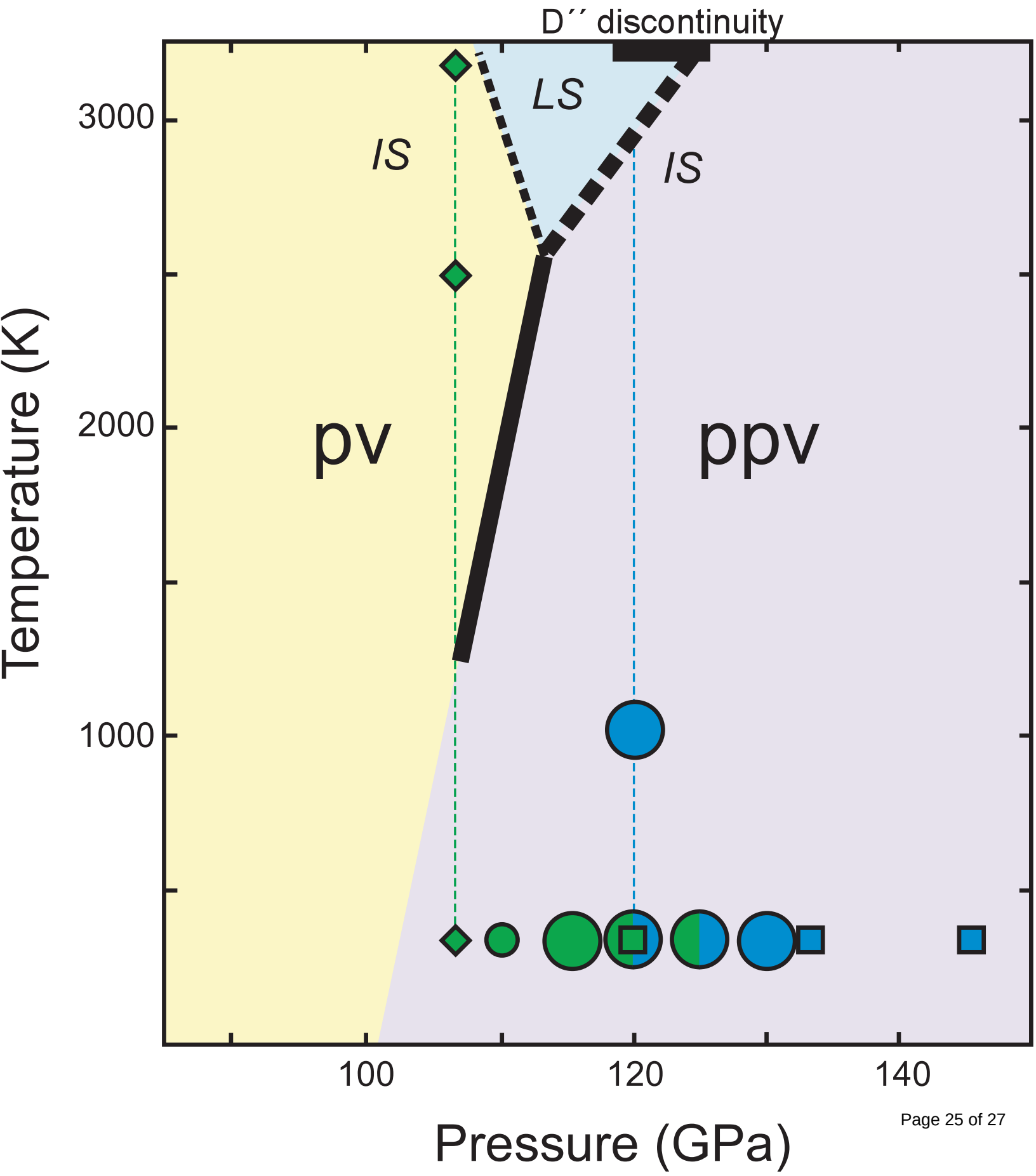

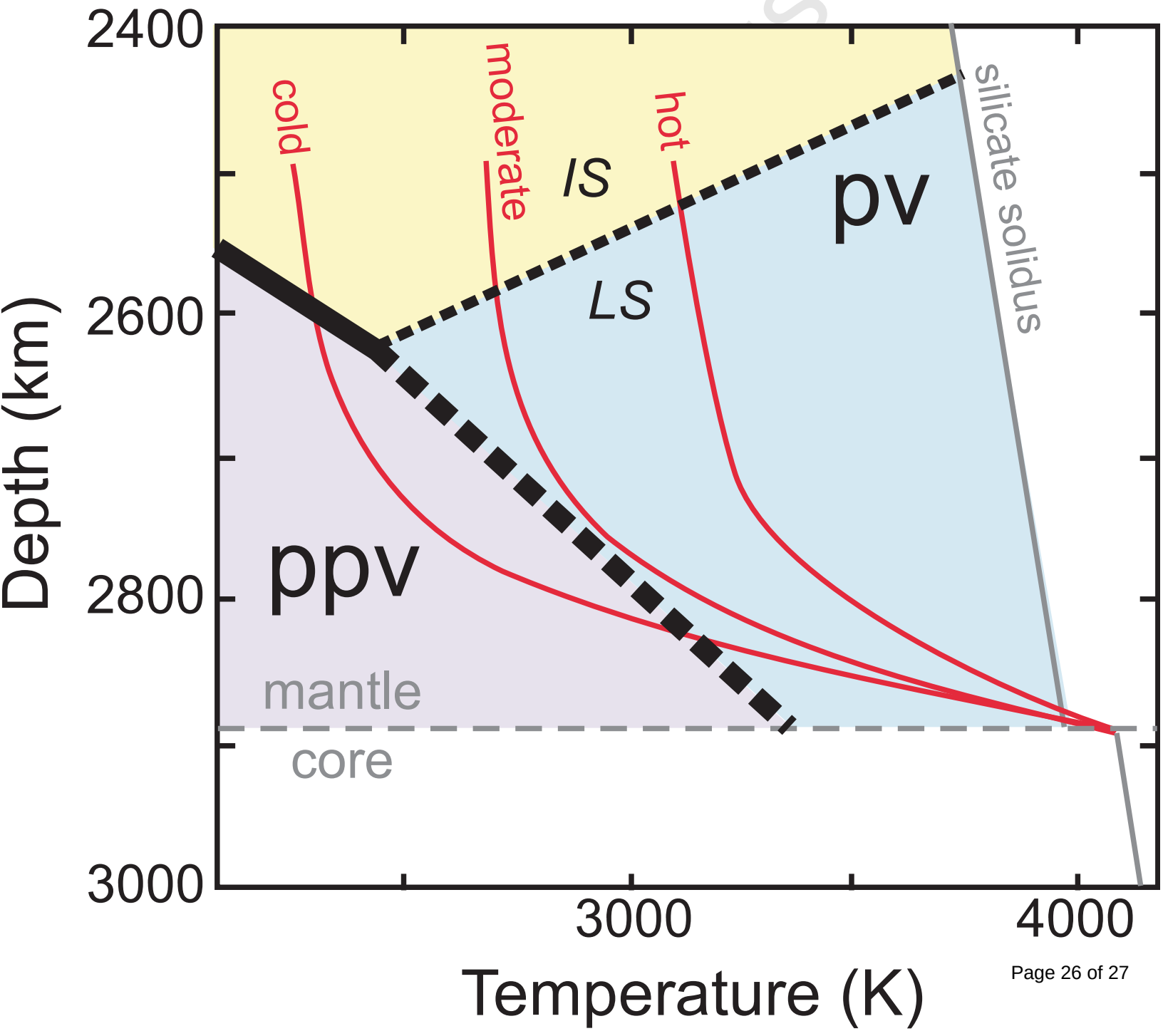

Table 1. Summary of run conditions and data collection

Run #	phase	P GPa	T K	NFS	Möss	comments
1	mj	0	300	x	x	
		33	300	x		LH at high power after data collection
	pv	33	300	x		
		40	300	x		
		49	300	x		
		62	300	x		
		74	300	x		
		89	300	x		
		115	300	x		
2	mj	0	300		x	
		39	300		x	
		61	300		x	
		145	300		x	LH at high power after data collection; P decreased during LH
	pv	125	300		x	
3	pv	120	300	x		
		120	380	x		DAC screws were tightened during heating to maintain constant P
		120	830	x		" "
		120	1000	x		" "
		130	300	x	x	P increased during quenching to room temperature

Notes:
mj: majorite; pv: perovskite; NFS: nuclear forward scattering; Möss: Mössbauer spectroscopy; LH: laser heating
During runs #1 and #2, the sample was annealed after each increase of pressure using an infrared laser at low power to relieve stress